FRIEDRICH-ALEXANDER
UNIVERSITÄT
ERLANGEN-NÜRNBERG

Fraunhofer
UMSICHT

Optimization of ammonia recovery from pyrolysis gases

Bachelor thesis

Do, Thi Khanh Huyen

23 September 1997

in

Bac Giang, Viet Nam

Supervisors: Prof. Dr. Andreas Hornung
Dr. Sophie Schönfeld

Commencement of work: March 1st, 2023

Bachelor thesis submitted to the examination board on: August 1st, 2023

Statutory Declaration

I confirm that I have written this thesis unaided and without using sources other than those listed and that this thesis has never been submitted to another examination authority and accepted as part of an examination achievement, neither in this form nor in a similar form. All content that was taken from a third party either verbatim or in substance has been acknowledged as such.

Erlangen, July 31th 2023

Acknowledgments

First of all, I would like to send the special thank to Prof. Dr. ANDREAS HORNUNG for taking over the internal supervision so that my external bachelor thesis was made possible.

I would like to thank Dr. SOPHIE SCHÖNFELD, my direct supervisor at the Fraunhofer Institute, who supported me on this topic from the start, who encouraged and supported me in implementing my ideas and gave me professional advice.

Furthermore, I would like to express my gratitude to my colleagues and fellow students at the Fraunhofer Institute, who fostered a friendly and supportive working environment and from whom I gained valuable insights into my research field.

I am also deeply thankful to all the professors at Friedrich-Alexander University for their invaluable lectures, which provided significant support throughout the process of writing my thesis.

Lastly, I would like to extend a heartfelt appreciation to my mother, father, sister and brother, and best friends for their unwavering support and encouragement in pursuing my passion.

Table of Contents

Acknowledgments 5
Abbreviation 7
1. Introduction 8
1.1. The TCR® Technology 9
1.2. Ammonia in the natural nitrogen cycle 10
1.3. Motivation 12
1.4 Materials and Methods 13
2. Results and Discussion 15
Trial 1 – T1 (beef manure, 700 °C) 19
Trial 2 – T2 (sewage sludge, 500 °C) 22
Trial 3 – T3 (hop spent grain, 750 °C) 23
Trial 4 – T4 (residual waste, 650 °C) 24
Trial 5 – T5 (hop vine chaff, 500 °C) 25
T5.1. Ammonia recovery from the wash bottle 25
T5.2. Solubility experiments 26
Trial 6 – T6 (hop vine chaff, 750 °C) 26
Trial 7 – T7 (Recrystallization) 28
Trial 8 – T8 (sewage sludge, 550 °C) 30
Trial 9 – T9 (Ammonia recovery from TCR® water in T1) 30
T9.1. Reaction with phosphoric acid 85% (17.3 M) 30
T9.2. Reaction with phosphoric acid 4.0 M 32
Conclusion and Outlook 35
Experimental 37
References 42

Abbreviation

MAP	Mono ammonium phosphate
DAP	Diammonium phosphate
TCR®	Thermo-Catalytic Reforming ®
EtOAc	Ethyl acetate
EA	Elementary analysis
RT	Reforming temperature
CR	Conversion rate
GC	Gas chromatography
UMSICHT	Umwelt-, Sicherheits- und Energietechnik

1. Introduction

Environmental destruction is one of the most important issues of the last few years, which has led to the production of energy from renewable resources and the development of sustainable technologies. Two major advancements are in the fields of solar and wind energy.[1-2] However, they cannot ensure a stable supply of electricity generation due to the fluctuation of the weather conditions and the sunshine duration.[3] Therefore, using other sustainable resources, which depend less on the weather conditions, is required. An attractive alternative: biomass can also be used to generate energy, to produce chemicals, or to provide liquid biofuels *via* biological,[4-6] thermal, and physical processing.[4, 7-11] Biomass conversion with thermal processes seems to be attractive for production due to its high efficiency and wide range of products with many applications. On the contrary, biological processes that form specific products such as biogas or bioethanol present a lower efficiency due to their long operation time.[7]

There are several methods of thermal conversion processes, such as fast pyrolysis, intermediate pyrolysis, slow pyrolysis (carbonization), and gasification. The detailed operating conditions of each thermal conversion process are given in Table 1.

Table 1: Operate conditions of different thermal conversion processes and the typical product weight yields with dry wood as feedstock.[9, 12-13]

Mode	Operate conditions[9]			Products [%][12]		
	Operating temperature [K]	Heating rates [K s^{-1}]	Residence time [s]	Liquid	Solid (char)	Gas
Fast	673-823	500	0.5-2	75	12	13
Intermediate	673-823	10-100	240-600	50 (in 2 phases)	25	25
Slow	673	up to 50	hours to weeks	30	35	35
Gasification	1023-1173	-	-	5	10	85

The properties of a particular feedstock, such as the heating value, residual moisture content, and ash melting point, are the key factors in choosing a process for biomass conversion.[14] It must be considered which operating conditions are optimal for desired products depending on the characteristics of the given feedstocks. For instance, some organic waste residues cannot be effectively converted with fast pyrolysis and gasification due to their low heating value,

which can result in poor-quality products. Furthermore, highly oxygenated liquids produced with these methods must go through further steps of catalytic upgrading due to their corrosivity and viscosity before they can be used as fuels. The potential of tending to polymerisation makes this kind of product unstable for application as an energy carrier.[15-17] For the feedstocks with high water content, high energy input is needed to evaporate the water, which makes the process inefficient. Moreover, the water vapor at high temperatures will lower the thermal efficiency.[3, 18] Low ash melting point can also cause issues at high operation temperatures, leading to ash slagging or agglomeration, [14-17] and can facilitate the formation of low-priced tars and bitumen.

1.1. The Thermo-Catalytic Reforming® (TCR) Technology

The idea to convert the biomass with intermediate pyrolysis was implemented by installing the patented Thermo-Catalytic Reforming reactor (TCR®) at Fraunhofer Institute for Environmental, Safety and Energy Technology UMSICHT branch Sulzbach-Rosenberg, Germany.[18] The TCR® reactor is based on the pioneered intermediate pyrolysis Haloclean and Pyroformer reactors to convert plastics, and waste biomass, respectively.[9, 19-20] As the name implies, the TCR® combines the intermediate pyrolysis with the subsequent catalytic reforming. MAHMOOD *et al.* first performed this concept successfully with brewer's spent grain.[21] The TCR® reactor can process various residues, including sewage sludge, plastics, residual waste, electronic scrap, and agricultural residues such as slurry or plant remains. The feedstocks must contain at least 70 wt% dry matter content in order to be able to be processed with the TCR® plants.

In the first stage of intermediate pyrolysis, the pre-drying biomass is added to the reactor *via* a hopper to a metal bunker. The feedstock is conveyed with the aid of the screw reactor, which not only enables the transport of the feedstock but also helps control the residence times of the feedstock in the pyrolysis stage.[22-23] Afterwards, the solid is led directly to the post-reformer, while the pyrolysis gases flow through the packed char bed. That facilitates the iterated contact of the pyrolysis gases with the formed char, which also serves as the reforming catalyst. The reforming step is necessary to improve the product's quality and to prevent the formation of tar and other harmful substances. The auger reactor and the post-reformer are electrically heated using external heating mantles.[24] The TCR® liquids, containing the TCR® oil and TCR® water, condensate at about 273 K[13] to separate them from the non-condensable gases such as carbon dioxide, carbon monoxide, a small amount of ammonia, hydrogen sulfide, and short-chain hydrocarbons like methane, ethane, etc. After the post-reformer is conveyed to the char collecting tank using the screw reactor, the formed char is formed. The energy contained in the gas can be converted directly into thermal energy for

other purposes like warming up the feedstocks. Otherwise, the hydrogen-rich syngas can be purified further and used as the potential feed of several synthesis reactions.[24] The conversion of biomass and all kinds of residues with the TCR® technique has the potential to regenerate energy carriers in the different forms of biochar, bio-oil, and hydrogen with near-zero emissions and contribute to reducing CO_2 emissions.[25]

The TCR® plant used in this work is shown in Figure 3 in the section "Materials and Methods". A simple schematic of the TCR® reactor is outlined in Figure 1.

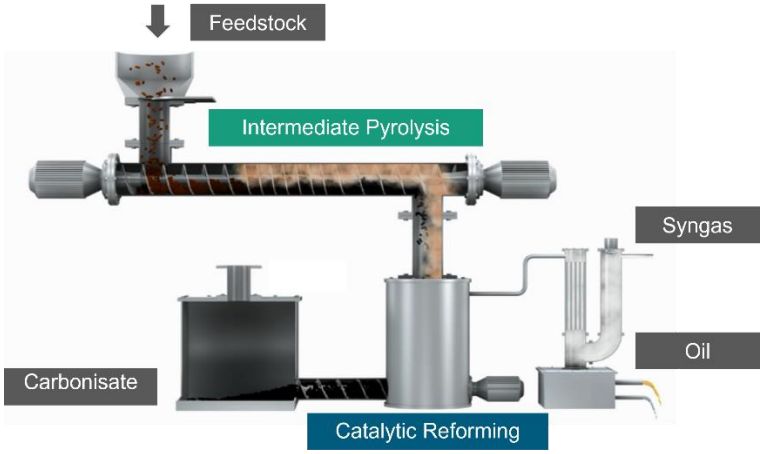

Figure 1: Schematic of the TCR® reactor. (©Fraunhofer UMSICHT)

1.2. Ammonia in the natural nitrogen cycle

In the natural nitrogen cycle, reactive nitrogen in the form of nitrate (NO_3^-) or ammonium (NH_4^+) enters the soil primarily through the decomposition of biomass utilizing the microorganisms' activities. In addition, reactive nitrogen can also be produced by lightning or volcano activity, whereas the stable triple bond of the elementary nitrogen molecules is broken.[26] Plants can directly use the water-soluble ammonium and nitrate from the soil as nutrients. Some of them, which have a symbiosis with specific bacteria such as cyanobacteria, can fix nitrogen from the atmosphere in the form of organically bonded $HCNH_2$.[26] On the ground, this organic nitrogen can be degraded into ammonium and converted into nitrate through nitrification in the soil. In this way, these plants can provide nitrogen themselves and enhance the soil's quality with reactive nitrogen. Through microbial denitrification, nitrate on the ground is converted into gaseous N_2O or N_2, which is released into the atmosphere, closing the nitrogen cycle.[26] Consequently, the nitrogen is lost from the biosphere and enters the atmosphere. The nitrogen cycle in the biosphere is illustrated in Figure 2.

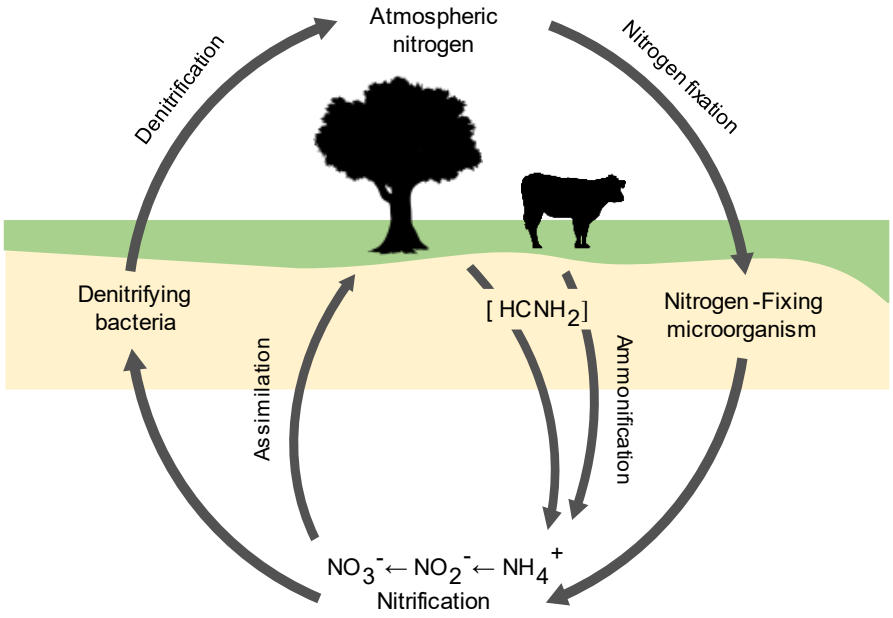

Figure 2: The natural nitrogen cycle. [26-27]

Converting the nitrogen from the atmosphere requires a lot of energy or specific bacteria with several steps to form reactive nitrogen. Hence, nitrogen in plant-available form is limited, and the nutrients provided by the natural nitrogen cycle in the soil are insufficient to meet their needs.[26] Therefore, targeted fertilization in agriculture is required.

Nitrate which is applied in the soil through fertilizer, can be lost from the biosphere through denitrification, evaporation into gaseous forms, or washing into surface and groundwater.[26] The nitrogen loss depends on several factors, such as soil properties, fertilizer application, and weather conditions.[26] Therefore, it is not always possible to prevent nitrate from washing out of the soil and entering groundwater.

1.3. Motivation

As mentioned above, other possible sources of nitrogen in the biosphere can be generated through decomposition of plant remains or cattle manure in the field. However, applying manure, a fixed mixture of nutrients, directly to the soil on farms is in some cases insufficient since it cannot be targeted to specific areas for a particular plant and the nitrogen loss can occur through ammonia evaporation. Furthermore, the organic residues cannot be left on the fields for an extended period due to the risk of groundwater pollution resulting from the supersaturation of nitrates and phosphates in the soil.[3, 28-30]

In order to produce nitrogen fertilizers from elemental nitrogen, it must go through the intermediate stage of ammonia synthesis. In the agricultural sector, ammonia plays a significant role as it is utilized in manufacturing of all mineral nitrogen fertilizers. Around 70% of annually produced ammonia is used in the manufacture of nitrogen fertilizers (IEA 2021).[31] In addition, ammonia is also employed in various industrial applications, such as synthetic fibres, explosives, plastics[31] and for storing energy, for example, as a hydrogen storage compound.[32-33]

In the 1900s, a modern industrial-scale ammonia synthesis process, the Haber-Bosch process, was successfully implemented,[34] which played a crucial role in helping humanity overcome the food crisis of that time by producing nitrogen fertilizers on a large scale.[35] The process involves synthesizing ammonia from its elements: nitrogen from the atmosphere and hydrogen from methane via steam-reforming, which is energy- and emissions-intensive. According to the report of the International Energy Agency in 2021, the ammonia production consumes around 2% of total energy for production worldwide and accounts for 1.3% of worldwide CO_2 emissions.[31] Considering the current perspective, reducing greenhouse gas emissions is increasingly important.

Therefore, it is crucial to regain ammonia from other possible sources to neutralise the energy expenditure put into ammonia synthesis and to minimise nitrogen loss from thermal conversion process of biomass. Instead of converting the energy contained in the process gas into thermal energy through combustion, ammonia gas can be recovered in the form of valuable substances, such as fertilizers. Furthermore, the ammonia recovery step can serve as an intermediate gas purification process. In the TCR® process, a fair amount of hydrogen can be generated which is possible to use for ammonia production after gas purification. Moreover, a small amount of ammonia is present in the gases, which can be continuously removed during the trials and recovered in a directly usable form.

This work aims to optimize the ammonia recovery from the pyrolysis gases, quantitatively and qualitatively, allowing the obtained product to be used for further applications without excessive energy input. Additionally, the influence of the post-reforming temperature on the yield will be discussed. Finally, a method for recovering ammonia from the aqueous solution was investigated.

1.4 Materials and Methods

The TCR®-2 plant, which has a throughput of 2 kg h^{-1} and is used to produce TCR® gas, TCR® liquid, and char on a laboratory scale, is shown in Figure 3. In this study, seven experiments were carried out with the TCR®-2 plant. The pyrolysis temperature was maintained at 450 °C, while the reforming temperature varied from 500 °C to 750 °C.[22] Nitrogen is flushed through the plant before the experiment to create an inert environment for pyrolysis.[13]

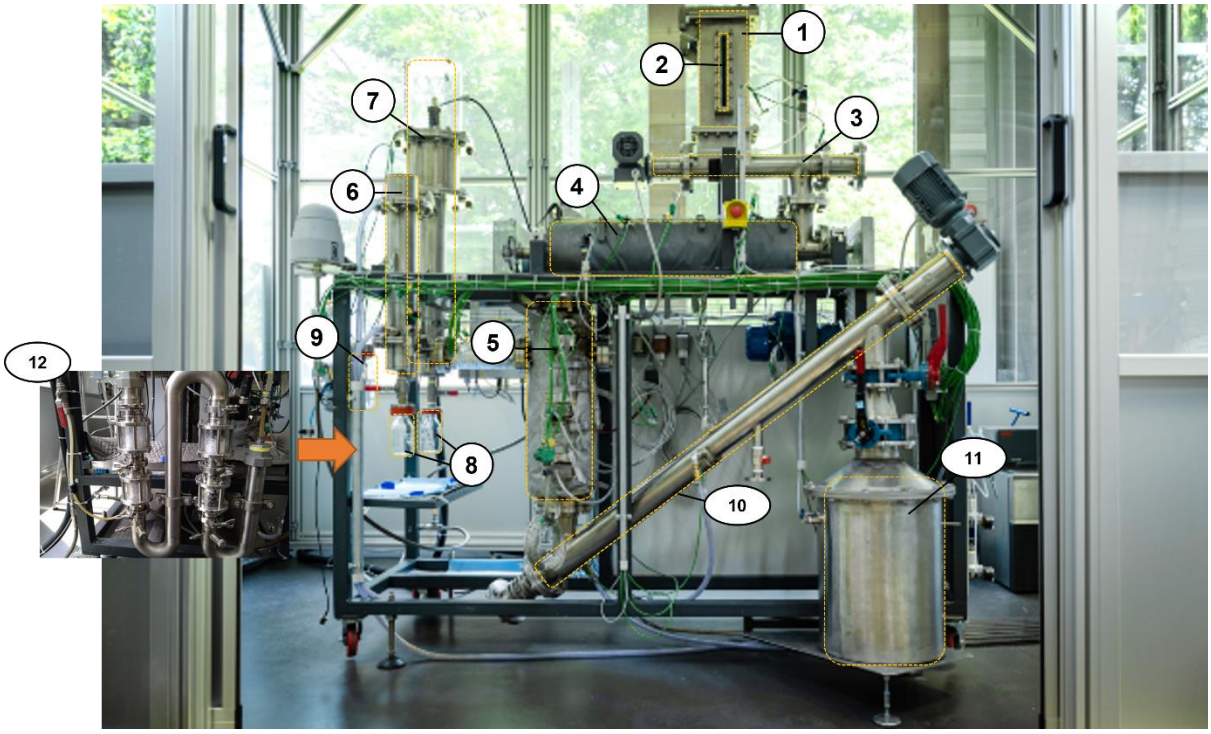

Figure 3: TCR®-2 plant at the ©Fraunhofer Institute UMSICHT, Sulzbach-Rosenberg with the components: (1) metal bunker, (2) vision panel, (3)(10) screw reactors, (4) auger reactor for pyrolysis, (5) post-reformer, (6) condenser, (7) electrostatic cyclone precipitator (ECP), (8) collecting glass bottles for condensate, (9) wash bottle, (11) char collecting tank, (12) bypasses.

Before the gases pass through the gas counter, an upstream wash bottle filled with water will prevent any harmful substances from contaminating the gas counter. A metal pipe is used to allow gases to encounter the liquid surface, which must be filled with at least 0.5 L of water. Cylindrical pistons with a maximum volume of 0.3 L each are installed in the bypasses, which

are connected in succession for ammonia removal from gases. The wash bottle and the bypasses were utilized as the ammonia removal and recovery units, which are highlighted in Scheme 1.

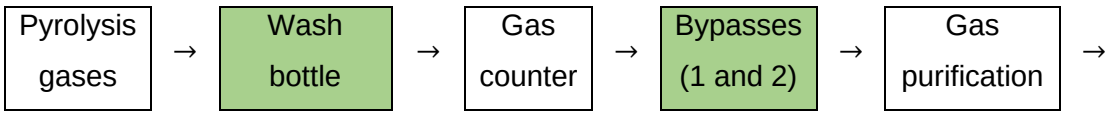

Scheme 1: Operating segments of ammonia recovery units.

For ammonia removal, phosphoric acid is used as a reacting agent with ammonia in the pyrolysis gases. The experiments were carried out with concentrated phosphoric acid (85%) and diluted phosphoric acid[36] in the total operating time. The gaseous ammonia was converted to mono ammonium phosphate (MAP), which can be utilized directly as nitrogen and phosphate fertilizer. MAP is water-soluble and will therefore immediately plant available in well-drained soils. When dissolved in water, MAP provides two ions which are important for plant growth: NH_4^+ and $H_2PO_4^-$. Also, a slight acid pH-value of MAP (4 to 4.5) is favourable in neutral and high pH soils by reducing the risk of NH_3 loss to the air.[37]

After ammonia is removed from the pyrolysis gas by washing with phosphoric acid, different processes for recovery solid MAP were implemented, such as adding organic solvents to precipitate solid MAP,[38] crystallizing over vacuum drying, and nucleation of MAP.[39]

Moreover, it is crucial to determine the nitrogen content of the feedstocks beforehand to ascertain the conversion rate, and the product yields afterwards. In this study, various kinds of feedstocks were converted: beef manure, sewage sludge, hops (hop vines chaff and hop spent grain), and residual waste. Sewage sludge and hop vines showed the highest nitrogen content of 3.6%[30] and 2% in dry mass,[40] respectively. Another feedstock, beef manure, has an average nitrogen content of 3.1% for composted and 2.2% for non-composted manure.[41] The nitrogen content of the manure may decrease due to ammonia volatilization during pelleting or other thermal treatments. Determining the nitrogen content of residual waste is challenging due to its mixture of various waste materials.

Chemicals and Equipment

All the equipment used in the experimentation were available at the Fraunhofer Institute UMSICHT.

Gas chromatography: The components are originally from *Agilent Technologies* and installed by *Teckso GmbH*. Agilent 8860 GC-System with a Gaspro column and a FID detector to detect carbohydrogens, a Volamin column and a WLD detector for analysing CO_2, NH_3, H_2S and H_2O and a MS5A column with a second WLD detector to detect H_2, N_2, O_2, CO and CH_4.

Heating mantel: WHM Heating Jacket for round flasks from *witeg Labortechnik GmbH*.

Rotary evaporator: The model Rotavapor® R-100 from *BÜCHI Labortechnik GmbH*.

The chemicals used were obtained from *Merck KGaA, PanReac AppliChem., Sigma Aldrich* These were used without further purification unless otherwise mentioned.

2. Results and Discussion

In this section, the results of the commissioning on the TCR®-2 plant with the extended bypass are presented and discussed in detail. To identify $NH_4H_2PO_4$ (MAP), a N/H ratio of 1:6 is expected, which can be calculated from the elementary analysis's results (Table 4). In elementary analysis, the percent composition of N, H, C and S in the obtained compounds are measured. The presence of impurities in the products, such as polymerised by-products, can be estimated by the deviation from the N/H ratio and the measured carbon content. The yields and the ammonia content in the gases can be determined using gas chromatography (GC).

Regarding GC analysis results, the pyrolysis gases contain H_2, H_2S, N_2, CH_4, CO, CO_2, NH_3, and hydrocarbons like short alkanes and alkenes, whereas most of N_2 content was applied from external tanks for flushing the plant. The gases are produced based on the equilibrium reactions (Eq. 1 - Eq. 6). As the endothermic reaction progresses, the equilibrium shifts towards higher temperatures. In this instance, the higher the temperature, the more gases produced. That is consistent with experimental results demonstrating increased gas yield at higher reforming temperatures. Besides, the solid and liquid yields decrease slightly under these conditions.[24] This process allows for the production of hydrogen through the following reactions:[13]

$CO_2 + C \rightleftharpoons 2CO$	$\Delta H = +172$ kg mol^{-1}	Eq. 1
$C + H_2O \rightleftharpoons CO + H_2$	$\Delta H = +131$ kg mol^{-1}	Eq. 2
$C + 1/2\ O_2 \rightarrow CO$	$\Delta H = -111$ kg mol^{-1}	Eq. 3
$CH_4 + H_2O \rightleftharpoons CO + 3\ H_2$	$\Delta H = +206$ kg mol^{-1}	Eq. 4
$CO + H_2O \rightleftharpoons CO_2 + H_2$	$\Delta H = -41$ kg mol^{-1}	Eq. 5
$C + 2H_2 \rightleftharpoons CH_4$	$\Delta H = -75$ kg mol^{-1}	Eq. 6

The first aim of this work is to enhance the yield of the ammonia recovery from the pyrolysis gases. Previous works in the institute has shown that ammonia could be absorbed in the impregnated phosphoric acid on perlite, an amorphous porous volcanic glass. However, the formation of contaminants resulting from the polymerization of organic components in the pyrolysis gases was unavoidable. The product yields resulted under 5%.[42] Due to the low concentration of ammonia in the gases, approximately 1-3% depending on the feedstock,

ammonia must be reacted selectively, that lead to different choices of reacting agents. After a certain product yield is achieved, the second aim of this work is to enhance the product's quality.

The formation of MAP from ammonia gas and phosphoric acid is shown in Eq. 7. Once the supersaturation of MAP is reached, the formation of diammonium phosphate (DAP) occurs promptly as the concentration of absorbed ammonia in the acid solution increases (Eq. 8). In the case of diluted phosphoric acid (as an reactant), the formed MAP will not crystalized due to its high solubility in water (at 25 °C, MAP: 400 g/L, DAP: 695 g/L).[39]

$$NH_3\ (g) + H_3PO_4\ (aq) \rightarrow NH_4H_2PO_4\ (s) \qquad \text{Eq. 7}$$

$$2\ NH_3\ (g) + H_3PO_4\ (aq) \rightarrow (NH_4)_2H_2PO_4\ (s) \qquad \text{Eq. 8}$$

The overview of all experiments conducted using phosphoric acid in the ammonia recovery units, wash bottle and bypasses, is shown in Table 2.

Table 2: Overview of all ammonia recovery units used in this work, which were carried out with different feedstocks at different post-reforming temperatures.

Trial	Feedstocks	m_{Feed} [g]	Post-Reforming temperature [°C]	Recovery units	
				Wash bottle	Bypass
T1	beef manure	6000	700	H_2O	H_3PO_4 (85%)
T2	sewage sludge	9000	650	H_2O	H_3PO_4 (4.0 M)
T3	hop spent grain	8000	750	H_2O	H_3PO_4 (4.0 M)
T4	residual waste	6000	650	H_3PO_4 (4.0 M)	H_3PO_4 (4.0 M)
T5	hop vine chaff	8618.7	500	H_3PO_4 (4.0 M)	not used
T6	hop vine chaff	9318.5	750	H_3PO_4 (4.0 M)	not used
T7	Recrystallization of the obtained product from T3				
T8	sewage sludge	10000	550	H_3PO_4 (4.0 M)	not used
T9	Ammonia recovery from TCR®-water T1				

In Table 3, the conversion rates and the yields based on the obtained products are calculated. It is assumed that the obtained product contained pure MAP.

The conversion refers to the amount of phosphoric acid used in the recovery units, which was converted to MAP.

$$Conversion\ rate\ (CR) = \frac{mole\ of\ obtained\ MAP}{mole\ of\ phosphoric\ acid\ in\ recovery\ units} = \frac{n_{MAP}}{n_{H3PO4}} \qquad \text{Eq. 9}$$

The product yield is defined by the quotient of the amount the converted MAP and the ammonia containing in gas, that can be deducted from Eq. 10.

$$Yield = \frac{mole\ of\ obtained\ MAP}{mole\ of\ ammonia\ in\ gas} = \frac{n_{MAP}}{n_{NH3,gas}} \quad \text{Eq. 10}$$

Table 3: Calculation of overall yields and conversion rates (CR: conversion rate). The same colour of the trials indicates the same/similar feedstocks.

Trial	**T1**	**T2**	**T3**	**T4**	**T5**	**T6**	**T8**
Feed	beef manure	sewage sludge	hop spent grain	residual waste	hop vine chaff	hop vine chaff	sewage sludge
RT [°C]	700	650	750	650	500	750	550
%NH_3, gas	1.33	2.99	1.07	2.00*	3.36	3.50**	3.31
m_{gas} [g]	2300.67	3941.90	4027.79	2109.67	3315.81	4481.24	3332.29
$m_{NH3,\ gas}$ [g]	30.64	117.94	43.02	42.19	111.38	156.84	110.30
$n_{NH3,\ gas}$ [mol]	1.80	6.93	2.53	2.48	6.54	9.21	6.48
n_{H3PO4} [mol]	3.47	1.20	1.20	2.20	2.00	2.00	2.00
m_{MAP} [g]	0	64.8	94.1	112.1	46.3	175.4	144.1
n_{MAP} [mol]	0	0.56	0.82	0.98	0.40	1.52	1.25
Yield [%]	**0**	**8.1**	**32.5**	**39.6**	**6.1**	**16.5**	**19.3**
CR [%]	**0**	**46.7**	**68.3**	**44.5**	**20.0**	**76.0**	**62.5**
obtained MAP	-					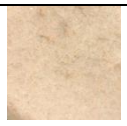	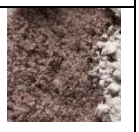

For two trials the measurement of the gas phase failed due to a malfunctioning GC system. Therefore, for these two trials an ammonia percentage was assumed.

* backed by literature it is assumed that at higher temperatures more ammonia is produced within the gas phase therefore an average amount of 2.0% is assumed.

** backed by literature it is assumed that at higher temperatures more ammonia is produced within the gas phase therefore a slightly higher amount than in T5 is assumed here.

In Table 3, trial 7 is not listed since it involved the recrystallization of the product obtained in trial 4. Also, since the measured values were taken before the bypass but after the wash bottle in trial 9, the yield cannot be determined.

In Table 4, the analysis results of the obtained products were consistent, which can be determined as MAP with the N/H ratio around 1:6. Despite the products' colouration, C and S content were mostly out of range and undetectable.

Table 4: Percent compositions of nitrogen, hydrogen, carbon, and sulfur in pure MAP compared with the obtained products of T1 – T9.

	N/H ratio	N [%]	H [%]	C [%]	S [%]
$NH_4H_2PO_4$	1:6	12.18	5.26	0.00	0.00
T1	-	-	-	-	-
T2	1: 6.2	11.89	5.27	1.28	0.01
T3	1: 6.1	12.01	5.30	0.19	0.02
T4	1: 5.8	12.44	5.20	0.18	0.00
T5	1: 6.3	12.14	5.49	0.20	0.02
T6	1: 5.9	12.16	5.48	0.09	0.00
T7	1: 5.9	12.43	5.25	0.06	0.02
T8	1: 6.0	12.35	5.27	0.10	0.00
T9	1: 6.0	12.34	5.22	0.16	0.00

The disadvantage of the trials is to convert different feedstocks with different amount at different post-reforming temperatures, which contains variable nitrogen contents. As a result, no correlation between temperature and ammonia concentration can be established. In addition, it is not possible to make an overall statement and comparison regarding the yield between the trials because of the transition of the recovery units; from the bypasses to the wash bottle.

In the following, a more detailed discussion for each trial with the subsequent laboratory analysis will be introduced. The detailed descriptions of the laboratory procedures will be presented in section "Experimental".

Trial 1 – T1 (beef manure, 700 °C)

The first trial was carried out at a post-reforming temperature of 700 °C with beef manure as a feedstock. Concentrated phosphoric acid (85%) was used as a reactant in both bypasses, whereas each was filled with 100 mL of phosphoric acid (85%). The gases first passed through bypass 1 and then bypass 2. Gas samples were collected before and after the bypasses for the GC analysis. After the trial, the reacting solution in the bypasses was collected separately in two glass bottles with a dark colour and fuel smell. Then, the precipitation experiments were carried out with two solvents: acetone and ethanol. A sample of each bypass (1 mL) was mixed in a sequence of increasing ratios with the solvents from 1:25 to 1:70 (Figure 4). It was observed in the sample from bypass 2 that black precipitation emerged at the ratio of 1:25. Colourless precipitation formed (Figure 5) up to a ratio of 1:50, which emerged more and more with the increasing amount of the solvents up to the ratio of 1:60. On the contrary, there are no changes observed during adding the solvents to the sample of bypass 2.

Figure 4: The precipitation experiment of the sample from bypass 1 with acetone in a ratio of (left to right) 1:25, 1:30, 1:35, 1:40, 1:45, 1:50, 1:55, 1:60, and 1:70.

The colourless solid was removed using a stirring rod to ascertain whether it was the desired product, MAP, by dissolving it in water. The remaining precipitation was filtered. As a result, it did not solve in water. The black precipitation stuck firmly to the filter paper and was greasy and not water-soluble. Due to the precipitation's properties and the solvents' expenditure, no product was obtained. The GC analysis results in Table 5 exhibited about 1.33% of ammonia content in pyrolysis gases.

Figure 5: Formed colourless precipitation.

Table 5: TCR® gas composition at 700 °C reforming temperature in T1.

Formula	Name	% Compound concentration	Formula	Name	% Compound concentration
CH_4	methane	10.199	C_6H_{14}	hexane	0.002
C_2H_6	ethane	0.648	C_6H_{12}	1-hexene	0.010
C_2H_4	ethene	1.364	C_7H_{16}	heptane	0.002
C_3H_8	propane	0.119	C_7H_{14}	1-heptene	0.007
C_3H_6	propane	0.716	C_5H_{10}	1-pentene	0.012
C_4H_{10}	butane	0.017	NH_3	ammonia	1.332
C_4H_8	1-butene	0.054	N_2	nitrogen	16.793
C_5H_{12}	pentane	0.006	H_2	hydrogen	27.452
CO_2	carbon dioxide	19.433	CO	carbon monoxide	8.890
			H_2S	hydrogen sulfide	0.176
Total					87.230*

*Some gases or water vapour are undetectable and account for the remaining percentages up to 100%.

The non-success of using concentrated phosphoric acid as the reacting agent forced us to find a more suitable substance for removing ammonia from the gas stream. On the one hand, at the high reforming temperature (700 °C), the gas stream would pass by the bypasses quickly, making a small reacting volume (100 mL each) even more insufficient. On the other hand, the acid solution would promote side reactions with the gaseous short-chain hydrocarbons, which mostly contained in the pyrolysis gases.[2, 43] Their oligomerized products can be an explanation for the characteristic red-brown colouration and the fuel smell of the obtained reacting solution. A range of different compounds can be formed through the oligomerization of light olefins, which had been investigated for production of “polymer gasoline”.[2, 44]

Previous work, in which the pyrolysis gases passed through phosphoric acid impregnated perlite and silica gel showed other organic impurities like acetonitrile, pyrrole and acetone were detected on the perlite’s surface. In the presence of acid, the polymerisation of pyrrole can occur leading to the formation of various compounds such as porphyrin, which explains the red or rust-brown colouration of the obtained reacting solution.[45] The side-reaction of pyrrole with acetone was performed at the institute’s laboratory. The emergence of the rust-brown product had confirmed the mentioned conjecture.[46] The chemical structural formula of pyrrole and porphin, the parent porphyrin, are illustrated in Figure 6.

a) b)

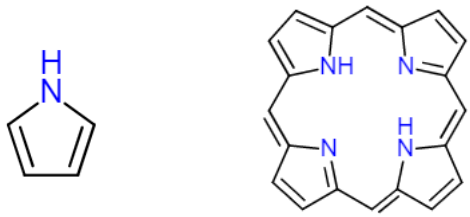

Figure 6: chemical structures of a) pyrrole. b) porphin, the parent porphyrin

Since the side-reactions are unavoidable, a more selective reacting reagent toward ammonia is considered, so that the concentration of hydrocarbons absorbed in the recovery units can be reduced. Because of these requirements, diluted phosphoric acid was used, in which the hydrocarbons are mostly insoluble. In contrast, ammonia is very soluble in water (the solubility of NH_3 at 20 °C is 541 g/L[47]). Additionally, an optimal concentration of phosphoric acid is required to reach the maximum reaction rate despite limited filling capacity of the bypass (0.3 L).

According to laboratory experiments of DONG *et al.*,[36] the highest absorption efficiency within a stripping process (98.7%) showed at the phosphoric acid concentration of 4.2 M with the solution volume of 40 mL. The improvement of the ammonia absorption has been shown by increasing the reacting (absorbing) volume instead of increasing its concentration.[36] That can explain the failure of trial 1 with concentrated phosphoric acid (85%, 17.3 M in 100 mL). Scaling it up for a volume of 300 mL, the similar concentration of 4.0 M is appointed to test the absorbing and reacting ability of the dilute phosphoric acid compared to the concentrated acid solution in trial 1, whilst taking into account the small amount of ammonia containing in the gas stream, different gas flow rate and different gas composition.

Trial 2 – T2 (sewage sludge, 500 °C)

In this trial, sewage sludge was converted at a reforming temperature of 500 °C. Phosphoric acid (0.3 L, 4.0 M) was filled in the first bypass and implemented for the total operating time (4 h). Once the trial had finished, the orange bypass solution was transferred to a glass bottle. Black impurities were formed on the liquid surface, which was filtered, and water was removed *in vacuo* until solid emerged in the round flask. In addition to the mostly formed white solid, some brown lumps emerged (Figure 7), which were ground into a fine powder and further washed with ethanol. The elementary analysis has shown that the N/H ratio in the product (1:6) corresponds to the expected ratio in the MAP.

Figure 7: Brown lumps formed during water evaporation.

As the result, 46.7% of the applied phosphoric acid has been converted with ammonia to MAP. Despite the low product yield (8.1%) the solid MAP was successfully obtained using phosphoric acid 4.0 M to obtain a white solid (64.8 g) with a small amount of contamination (1.28% C content). It was observed that the colour of the obtained acid solution changed from red-orange to brown while removing water in the rotary evaporator at 95 °C, implying catalytic side-reactions over phosphoric acid. That explains the emergence of the brown lumps and the product's colouration. Hence, it is preferable to conduct the laboratory analysis immediately after completing the trial. Since a portion of the organic compound in the reacting solution is water-soluble, side reactions can take place under catalytic activity of acid solution over a long period of time.

In conclusion, the overall reacting efficiency was improved using the phosphoric acid (4.0 M), while only about half of the acid was converted. In the upcoming trial (T3), both bypasses were filled with 0.3 L phosphoric acid 4.0 M in order to increase the reacting volume.

Trial 3 – T3 (hop spent grain, 750 °C)

In this trial, hop spent grain was converted at a post-reforming temperature of 750 °C (Figure 8a). Both bypasses were filled with 0.3 L of H_3PO_4 4.0 M. At the onset of the trial, a significant formation of acid foam was observed (Figure 8b), resulting in the potential leakage of the acid from the bypasses into the pipeline and posing a risk of damage to the TCR® plant. The foam formation could be explained based on the base-acid exothermic reaction between ammonia and phosphoric acid (Eq. 7). The emerged water can be converted partly to steam, and the soluble process of gas compounds in the gas stream into the solution might involve in the foam formation due to the viscosity of the solution.

a) b)

Figure 8: a) hop spent grain pellets, b) Foam formation in the bypasses during trial T3.

Therefore, the phosphoric acid solution in bypass 2 was drained 10 minutes after the trial had started. Subsequently, only bypass 1 was utilized as the absorber for the remaining duration of the operation. The trial was carried out for 4 h. The absorbing acid solution was collected after the trial and processed according to previous trials described above to yield a brown solid (94.1 g, 32.5% yield). It is demonstrated that the conversion rate (68.3%) has been improved significantly compared to the last trial (46.7%).

However, the limited filling capacity of the bypass is still an issue as the reacting agent could not be filled in the second bypass. An applicable consideration of increasing reacting volume is using the upstream wash bottle, which was typically filled with water to catch harmful substances for the gas counter. Due to the high water-solubility,[47] ammonia can be absorbed in the aqueous wash bottle, reducing the initial amount of ammonia that passes through the bypasses. Therefore, the wash bottle was used in the next trial as an ammonia recovery unit, together with the first bypass, and filled with 0.5 L phosphoric acid 4.0 M.

Trial 4 – T4 (residual waste, 650 °C)

In this trial, the thermal conversion of residual waste was performed at the reforming temperature of 650 °C. In addition to previous experiments, a higher reacting volume was created by filling phosphoric acid 4.0 M in the wash bottle (0.55 L) and the first bypass (0.3 L). It was observed during the trial that the acid solution was turned from colourless to orange after 30 min and to red after 1 h of operating time. The trial was performed for 5 h. Following the trial, it remained about 0.3 L of reacting solution in the wash bottle after the organic impurities were removed. The wash bottle solution was dried out *in vacuo* to yield a pink solid (112.1 g, 39.6% yield).

In regard to the bypass's solution, the ammonium test paper from *MACHEREY-NAGEL GmbH & Co. KG* with the sensitivity limit of 10 mg/L NH_4^+ was used for the qualitative determination of ammonia in the reacting solution. The principle of the test is using Nessler's reagent,[48] mercury(II)-potassium-iodide, to react with ammonia in alkaline solution (NaOH) forming an intense brown precipitate.[49] As the test result, a light yellow spot has indicated a low concentration of ammonia, so that the bypass solution was not proceeded further due to the energy expenditure for removing water from the solution. A more detailed description of the test is presented in the section "Experimental".

Due to the technical issues, the NH_3 content could not be determined with the GC. Therefore, it was assumed that the produced ammonia accounted for 2.0% in the pyrolysis gas at a reforming temperature of 650 °C, resulting a good conversation rate of 44.5% and a slightly higher amount of product. The higher reaction volume appears to have a positive impact on ammonia recovery.

Trial 5 – T5 (hop vine chaff, 500 °C)

T5.1. Ammonia recovery from the wash bottle

Following the success of T4, the same strategy was utilized further to convert hop vine chaff at a post-reforming temperature of 500 °C. In this trial, the bypasses were not used regarding to the slight amount of ammonium contained in the bypass with the upstream acid wash bottle in T4. The wash bottle was filled with 0.5 L of H_3PO_4 4.0 M. Compared to T4, the same observation of the solution's colour change in the wash bottle occurred during the trial. After 5 h operating time, a red solution was obtained. The water was removed *in vacuo* to yield a pink solid (46.3 g, 6.1% yield).

Surprisingly, a much lower yield was obtained despite a longer operating time and a high ammonia concentration in gas stream (6.54 mol), which is comparable to that in T2 (6.93 mol). The conversion rate is also much lower than that in T2; only 20.0% phosphoric acid was converted into the obtained product. Aside from the reforming temperature, many other factors can affect the conversion rate and the yield such as pressure, gas composition, etc. To investigate the influence of the reforming temperature on the product yield, the same feedstock, hop vine chaff, was converted at a higher post-reforming temperature in the upcoming trial.

As an intermediate result, after conducting four trials using diluted phosphoric acid, the products were obtained with good yields and conversion rates. However, the contaminants present, which were formed at a high temperature for removing water (90 – 95 °C) and under the catalytic activity of phosphoric acid, could not be effectively washed out using organic solvents like ethanol and acetone after vacuum drying. To address this issue, a potential solution is to perform over liquid-liquid-extraction with another organic solvent that is immiscible with water and has better solubility for the contaminants, allowing them to be transferred from the aqueous phase. Choosing a suitable solvent can reduce the impurities from the products.

During these trials, it was observed that an organic layer formed on the surface of the acid solution, which can be removed by decanting. In the following subsection, the solubility experiments were performed to find a suitable solvent for the extraction process.

T5.2. Solubility experiments

Different solvents, such as n-hexane and ethyl acetate (EtOAc) were used for testing the solubility of the pollutants. Furthermore, the solvents such as tetrahydrofuran (THF), n-hexane, and EtOAc were tested for the liquid-liquid-extraction. In Figure 9a, it is obvious that the contaminant was soluble in EtOAc, but not in n-hexane. In Figure 9b, THF formed a homogeneous phase with the MAP solution and thus, it is also unsuitable for liquid-liquid extraction.

However, despite the solubility of the pollutants in EtOAc, the obtained product could not be washed further with EtOAc after washing it with ethanol (see Experimental, Laboratory analysis of trial T6). Therefore, the method proved unsuitable for the processing of other products.

a) b)

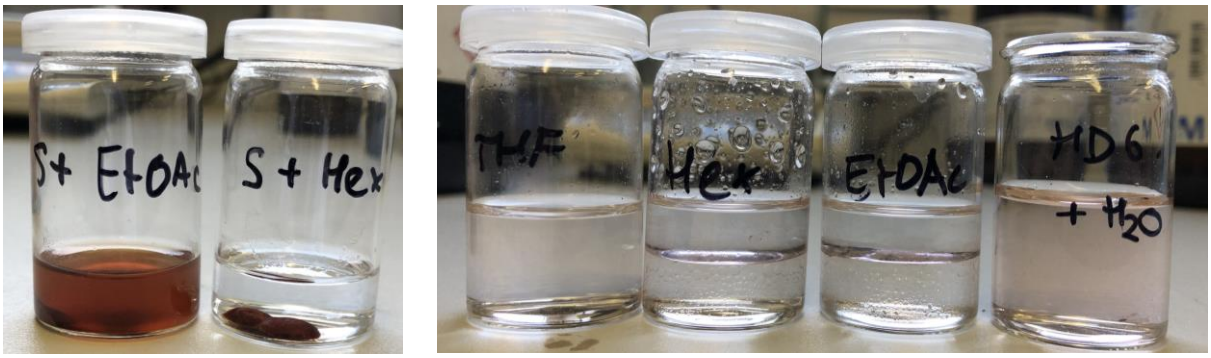

Figure 9: a) Organic impurity was dissolved in EtOAc (left) and n-hexane (right), b) liquid-liquid-extraction of the obtained product (right) in water with different solvents, from left: THF, n-hexane, EtOAc.

Trial 6 – T6 (hop vine chaff, 750 °C)

Hop vine chaff was converted at a post-reforming temperature of 750 °C. The wash bottle was filled with 0.5 L of H_3PO_4 4.0 M. After the trial, a light-yellow reacting acid solution was obtained. Interestingly, crystals formed in the filtrate after filtration (Figure 10), indicating the supersaturation of formed MAP in water (solubility of MAP in water: 368 g/L at 20°C[50]). The crystals were filtered and air-dried separately (17.1 g, fraction 1). The filtrate was then concentrated under reduced pressure. While the solution cooled down at room temperature, the crystallization in the round flask was observed. The formed crystals were taken out and

air-dried (97.5 g, fraction 2). The remaining solution was dried out completely *in vacuo* to yield as a light grey solid (60.8 g, fraction 3). Overall, 175.4 g was obtained from three fractions.

Figure 10: Formed crystals in trial 6.

Three obtained product fractions are shown in Figure 11.

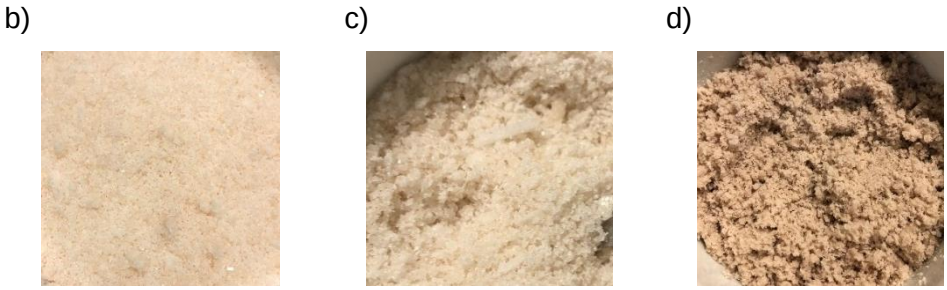

Figure 11: The obtained MAP in three fractions: fraction 1 (left), fraction 2 (middle), and fraction 3 (right).

Similar to the products of previous trials, the N/H ratio of the three fractions are around 1:6 with consistent analysis results (Table 6).

Table 6: Results of the elementary analysis of three fraction in T6.

	Fraction 1	Fraction 2	Fraction 3
N/H ratio	1: 6.3	1: 6.4	1: 6.2
N content [%]	12.14	12.12	12.22
H content [%]	5.48	5.54	5.43
C content [%]	0.13	0.08	0.07
S content [%]	0.00	0.00	0.00

Overall, a remarkable conversion rate of 76.0% and a good yield for ammonia recovery of 16.5% were obtained. Compared to T5, the conversion rate is clearly higher at a post-reforming temperature of 750 °C. The coloration of fraction 3, compared to fractions 1 and 2, provides strong evidence for the different product's quality achieved through crystallization

over vacuum drying and crystal growth. During vacuum drying, the solvent (water) can be completely removed, leaving behind the desired product with inseparable pollutants. In contrast, during crystal growth, the obtained product approximates the optical properties of pure analytical MAP (colourless crystals), and the pollutants are left in the crystal solution.

In conclusion, this experiment has demonstrated an alternative method for obtaining solid MAP from the solution through crystal growth, effectively reducing the products undesired colouration. Following this concept, the crystal growth was performed by recrystallizing the obtained product of T4 in the upcoming trial.

Trial 7 – T7 (Recrystallization)

The product of T4 was dissolved in water for recrystallization to eliminate the impurity causing the pink colouration. Regarding the solubility of MAP in water (368 g/L at 20 °C[50]), the remaining water had to be at least under 271 mL to facilitate the nucleation of about 100 g MAP at 20 °C, which can be achieved by removing water partly under reduced pressure. Once the supersaturation can be determined indirectly through the evaporated water, the nucleation of MAP was carried out, which are illustrated in Figure 12. 0.5 g of analytical MAP was implied evenly in the crystal bath. After 10 min, definitive crystal growth was observed that was allowed to crystallize overnight. Colourless crystals (87.3 g, 87.3%) were obtained.

The supersaturation grade (S) can be calculated with the following equation:

$$S = \frac{Volume\ of\ water\ needed\ to\ dissolve\ x\ (g)\ MAP}{Volumen\ of\ the\ current\ solution\ contained\ x\ (g)\ MAP} \qquad \text{Eq. 11}$$

$$= \frac{271\ mL}{(300 - 90)\ mL} = 1.3$$

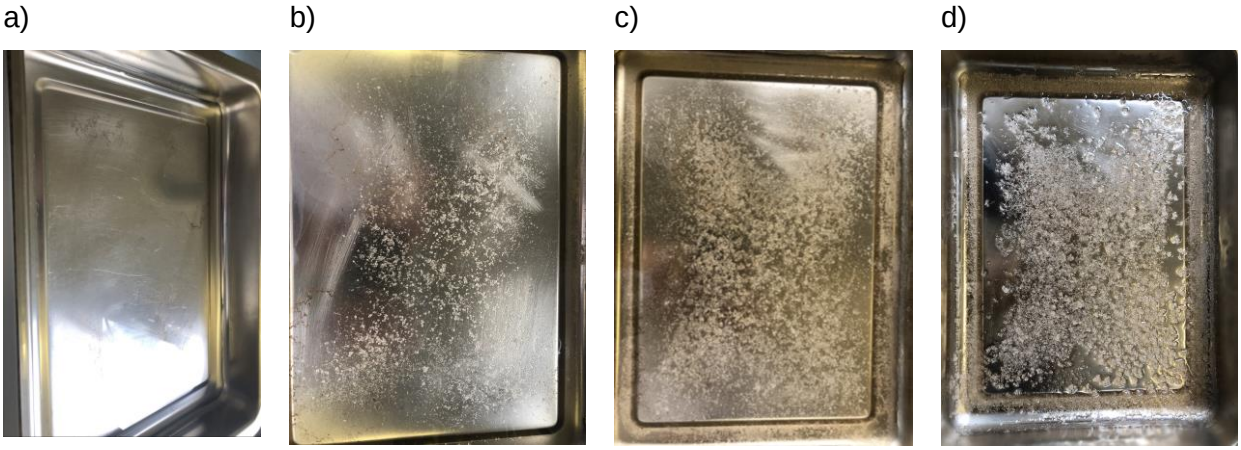

Figure 12: Crystal growth observation: a) at the beginning, b) after 10 min, c) after 30 min, d) overnight.

In general, there are no significant difference between these two samples after the recrystallisation regarding the analytical results (Table 7). The C content is slightly reduced. The measured values for the S content were outside the detection range and can be therefore neglected. It is convincing that the contaminants might be represent in very small amounts, but still can result an intense colouration.

Table 7: The obtained MAP before (left) and after (right) the recrystallization.

N/H ratio	1: 5.8	1: 5.9
N content [%]	12.44	12.43
H content [%]	5.20	5.25
C content [%]	0.18	0.06
S content [%]	0.00	0.02

The recrystallization yield might indicate the actual percentual amount of pure MAP contained in the obtained product. On the one hand, some contaminants were removed in the form of water-insoluble foam after the solid was dissolved in water. On the other hand, after the nucleation, a large amount of impurity and possibly a small amount of MAP was left in the remaining liquid in the crystallisation bath. Furthermore, less ethanol was used for washing the obtained product. From a broader perspective, the application of crystal growth is feasible on an industrial scale due to its ease of implementation that is currently used in the production of industrial fertilizers.[39]

To apply fertilizers in the field, their containing contaminants such as polycyclic aromatic hydrocarbons (PAHs) and heavy metals must be below their limit values, i.e., 0.1 $mg \cdot g^{-1}$ in Germany for the total amount of PAHs,[51] since they can cause a wide range of toxicity for human, animals, and the environment. Moreover, PAHs can be strongly adsorbed to soil,[52-53] so that the purification of coloured product before their application is required. The cost of these purification steps can be significant. If the coloured compounds already meet the required standards, these costs can be saved, which can be confirmed through further experiments.

Subsequently, the last trial with TCR®-2 plant was performed. In general, the reaction between of liquid and gas in the gas stream carries out mainly on the phase boundary between gas

and liquid. Therefore, a high surface is required to enhance the gas gas-liquid mass transfer.[54] To increase the two-phase boundary, plastic fillers were used to fill the acid surface in the wash bottle.

Trial 8 – T8 (sewage sludge, 550 °C)

In this trial, sewage sludge was converted at a post-reforming temperature of 550 °C. The plastic fillers were located in the wash bottle contained 0.5 L of H_3PO_4 4 M. After 5 h operating time, the absorbing solution was collected for further processing. The fillers were filtered together with organic impurities. To achieve a certain level of supersaturation and estimate the potential amount of MAP that could be obtained, the water was evaporated for 1 h. The crystal growth was conducted overnight to yield pink crystals and a white solid (144.1 g, 19.3% yield).

As the result, the nucleation was successfully performed. Less energy and less solvent were used compared to the previous trials. Besides, a good yield (19.3%) and a high conversion rate (62.5%) were obtained.

In the subsequent trial, the ammonia recovery from TCR® water is presented. After separation from the TCR® oil, the TCR® has shown a high nitrogen content, that can be qualitatively determined with ammonium paper test.

Trial 9 – T9 (Ammonia recovery from TCR® water in T1)

The concept of this experiment was vaporising ammonia from the aqueous solution, which was reabsorbed in the phosphoric acid in the gas washing bottle. The solution from the TCR® water in T1 was parted in two halves to compare the absorbing ability of concentrated phosphoric acid (17.3 M, 85%) and diluted phosphoric acid (4.0 M). The experimental setups were generally not different, which are shown in Figure 13 and Figure 15.

T9.1. Reaction with phosphoric acid 85% (17.3 M)

In Figure 13, the TCR® water was filled in a four-neck round flask (1). The dropping funnel (2) was filled with concentrated sodium hydroxide solution in excess to shift the equilibrium (Eq. 12) towards ammonia.

$$H_2O + NH_3 \rightleftharpoons NH_4^+ + OH^- \qquad \text{Eq. 12}$$

Using the thermometer (3) allowed the temperature control from outside. The round flask was heated with the heating jacket (4). The gaseous ammonia vaporized and was directed through the pipes to the washing bottles (6,8,9) through the plastic tubes (5). The washing bottles (6) and (8) were filled with concentrated phosphoric acid 85% and 4.0 M, respectively. The fillers were filled in these two washing bottles to create a larger reacting surface. The ice bath (7) was used for cooling off the reaction mixture due to the gas exothermic acid-base reaction between ammonia and phosphoric acid and the gas absorption. The washing bottle (9) was filled with phenolphthalein to indicate ammonia escaping from the washing bottle (8).

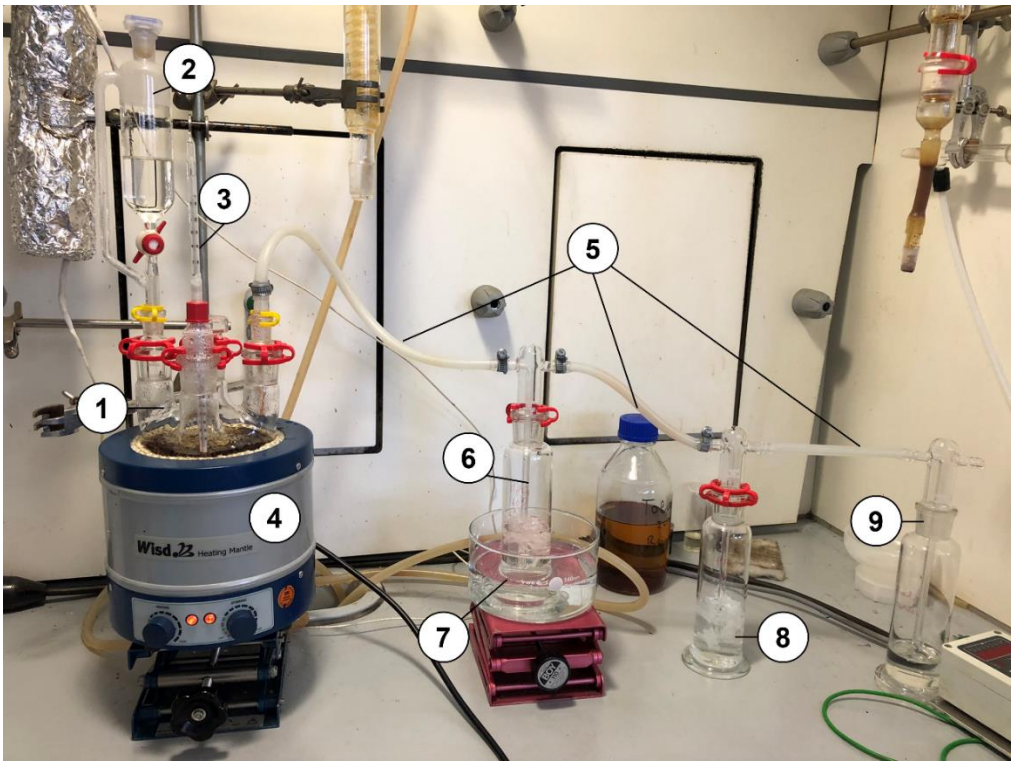

Figure 13: Experimental setup (T9.1) for ammonia recovery from TCR® water: (1) four-neck round flask, (2) dropping funnel, (3) thermometer, (4) heating mantel, (5) plastic tubes, (6) washing bottle filled with phosphoric acid 60% and plastic fillers, (7) ice bath, (8) washing bottle filled with phosphoric acid 35% and plastic fillers, (9) washing bottle filled with phenolphthalein 1 wt-% in ethanol.

At the beginning of the experiment, NaOH solution (50 mL, 10 M) was added dropwise under stirring into the TCR® water. As the solution's temperature reached 90 °C, the colour change in the washing bottle was observed, rapidly turning from colourless to yellow to orange to brown every 2 min (Figure 14). Accordingly, the temperature in washing bottle (6) increased. After 1 h, the qualitative ammonium tests were conducted, controlling the presence of ammonia in the original TCR®-water solution and the washing bottle (8). The test results showed that ammonia was totally desorbed from the round flask and solely absorbed in the

wash bottle (6). The indicator solution (9) also demonstrated that vaporized ammonia was absorbed in the upstream washing bottles. Hence, the experiment was terminated.

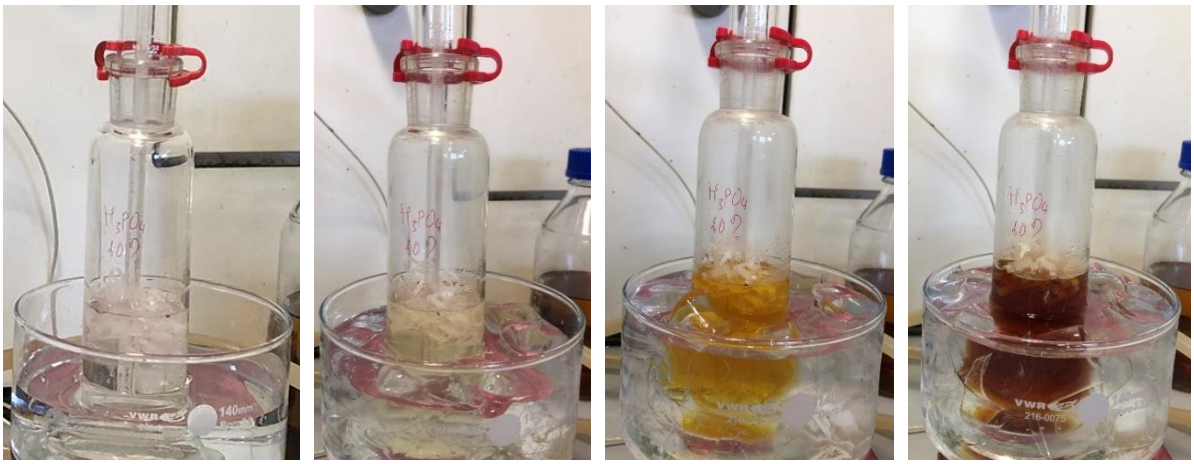

Figure 14: The colour change of the acid solution during the ammonia absorption every 2 minutes (left to right)

T9.2. Reaction with phosphoric acid 4.0 M

The concentrated phosphoric acid was not used in this attempt to investigate the colour change of the acid solution in dependence on the acid concentration. Instead, only diluted phosphoric acid (4.0 M) was filled in washing bottle (6) (Figure 15). A more straightforward experimental setup is shown in Figure 15. The same procedure as T9.1 was performed. Interestingly, no colour change was observed in the washing bottle containing 4.0 M phosphoric acid (6). However, the temperature of the absorbing solution remained nearly unchanged. No colour change was observed in the phenolphthalein solution (8). The experiment was conducted for 1 h, until ammonia was no longer detectable with the ammonium paper test.

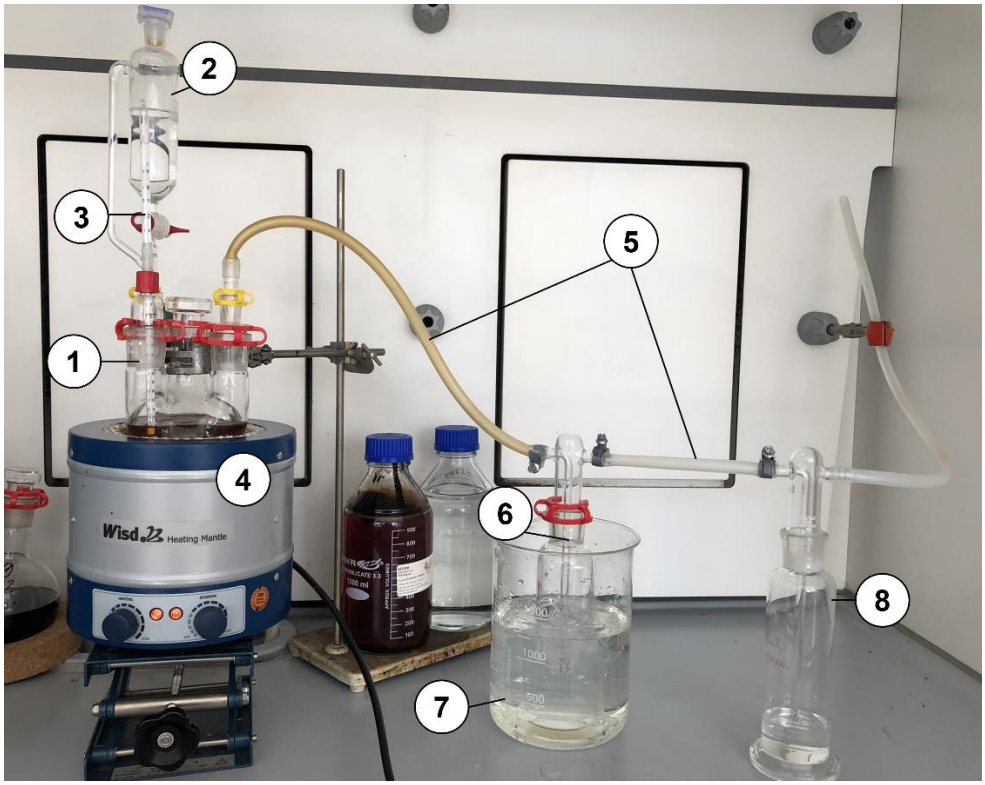

Figure 15: Experimental setup (T9.2) for ammonia recovery from TCR® water: (1) four-neck round flask, (2) dropping funnel, (3) thermometer, (4) heating mantel, (5) plastic tubes, (6) washing bottle filled with phosphoric acid 35% and plastic fillers, (7) ice bath, (8) washing bottle filled with phenolphthalein 1 wt-% in ethanol.

In conclusion, the experiments using concentrated (T9.1) and diluted (T9.2) phosphoric acid delivered the same results, indicating that the ammonia in the TCR®-water reacted with the acid solution. Nevertheless, the colour change observed in the concentrated phosphoric acid (17.3 M, 85%) has strongly supported the argument that it had the potential to absorb other vaporized components and catalyse side reactions. Furthermore, the water vapour was saturated in the concentrated phosphoric acid solution, causing the temperature increase besides the exotherm acid-base reaction. It has been shown that the heat management with an ice bath would not have been sufficient if the reaction had been performed for a longer duration. This issue was managed much better in T9.2 since water was a main component of the solution, allowing ammonia to be easily absorbed and a gradual reaction with phosphoric acid to take place. Besides preventing the superheating of TCR® water in the experiment with phosphoric acid 4.0 M, the solution's colour did not change during the experiment, enabling the recycling of the remaining acid.

The obtained absorbing solution of two attempts was combined for further processing to yield pink crystals and a white solid (98.4 g), whose N/H ratio, C and S content are comparable to

previous trials, while a significant lower energy input has been put in the system with shorter reaction time. The analysis results are given in Table 8.

Table 8: Analytical results of obtained product in T9

Conversion rate [%]	37.2
N/H ratio	1: 6.0
N content [%]	12.34
H content [%]	5.22
C content [%]	0.16
S content [%]	0.00

Conclusion and Outlook

In summary, the first aim of this work was achieved that the product yield has been improved for diverse feedstocks at the varied post-reforming temperature between 500 – 750 °C. It has shown that it is possible to recover ammonia partly from the pyrolysis gases regardless of the feedstocks. For further applications, the TCR® gas must be purified further to remove contaminants like ammonia and hydrogen sulfide. In this sense, the ammonia recovery can serve as an intermediate purification process, providing the benefit of obtaining fertilizers. Thus, the loss of valuable nitrogen during thermal conversion can be minimised.

The product yield was mostly obtained in the range of 20 - 40%, depending on the ammonia content in the pyrolysis gas, which in turn depends on the post-reforming temperature. The results regarding yield and conversion rate are not comparable between the trials, because different feedstocks were converted at the varied post-reforming temperatures. Varied modifications of the recovery units were carried out, from extended bypasses to the integrated wash bottle, that delivered consistent results though. The conversion rates of phosphoric were optimal at these high post-reforming temperatures, which were obtained over 40% at 650 °C and in the range of 68 to 76% at 750 °C.

The second aim of this work was also successfully carried out, improving the product's quality with crystal growth. Since the polymerization of organic contaminants was unavoidable and could not be eliminated by washing the obtained products, a more favourable method was sought in terms of product’s cleanliness and avoiding energy expenditure. Despite the consistent utilization of the acid recovery units, the evaporation of ammonia from aqueous wash bottle would be more economical. Furthermore, the contaminants could be reduced significantly based on the products’ optical properties. In order to investigate the potential for recycling phosphoric acid, the aqueous wash bottle should be used in further experiments. Rather than processing the wash bottle individually for each trial, combining the wash bottles from several trials would enhance the economic feasibility of ammonia recovery. On a larger scale, it would be advantageous to use a bigger stirred tank, taking into account improved stirring efficiency and better heat management or using plug flow reaction. Further experiments without using sodium hydroxide solution should be carried out to confirm its affect to the ammonia desorption from the aqueous solution.

Once ammonia has been absorbed in the acid solution, several methods can be employed to obtain solid MAP. Implementing a crystallization batch with an external cooling system can be considered for large-scale industrial applications. Otherwise, in order to reduce energy consumption and production costs through evaporation and cooling, a novel method of

antisolvent crystallization was investigated.[55-59] This involved adding an antisolvent, such as ethanol, to the crystallizer containing the precipitated MAP. The solid MAP can then be separated from the remaining fluid, allowing for the distillation of ethanol with a high concentration for recycling.[38]

For further prospect, using fillers to enhance the absorbing surface area might be an effective approach and might contribute to the enhancement the product yield. To address the contamination of plastic fillers, which were not reusable due to the polymerization of organic components in gases, an alternative approach involving the integration of a metal grid within the wash bottle can be considered. The advantages of using the wash bottle as an absorber compared to the bypasses was that a larger absorbing volume. Furthermore, the pressure drop of the piping bypass system could be an issue for operating a large-scale TCR® plant. To increase the absorbing ability of the wash bottle, it is feasible to construct a cascade of two to three wash bottles, each equipped with an integrated metal grid. The influence of using this wash bottle cascade should be experimented with to determine its effect on the production yield of other TCR® products, such as TCR® gas and liquid.

Experimental

Preparing of phosphoric acid 4.0 M: Phosphoric acid (69 mL, 85%) was added slowly under stirring to deionised water (231 mL).

Laboratory analysis of the trials T2-T5

All subsequent trials involved the same procedures, including gathering the gas sample for GC analysis, transferring the bypass solution into a glass bottle, filtering the absorbed acid solution to remove the water-insoluble layer, and removing the water *in vacuo*.

After filtration, water was removed *in vacuo* until the solid emerged (p = 380 mbar to 100 mbar, $T_{set,\ water\text{-}bath}$ = 95 °C). The obtained solid was washed with ethanol (50 - 100 mL). The formed lumps were ground into a fine powder. The combine solid was then suspended in ethanol (100 - 150 mL). The suspension was filtered. The solid was washed again with ethanol several times (each with 50 mL). The obtained solid was air-dried in a desiccator overnight.

Qualitative determination of ammonia with ammonium test paper

The pH value of the obtained acid solution was determined using indicator paper (typically pH = 1-2). One to two drops of the acid solution without pollutants were placed onto the test paper, and immediately afterwards, two drops of 10% sodium hydroxide were added. A colour change from yellow to deep brown, depending on the ammonia concentration, indicates the presence of ammonia in the solution.

Solubility experiments (T5.2)

2 g of the obtained product from T5.1 was dissolved in deionised water (30 mL) at 30 °C. Formed foam was removed. The obtained pink solution (5 mL each) was added to 5 mL of the solvents THF, n-hexane, EtOAc. The mixtures were then well mixed. The liquid phase boundary was observed in the sample of n-hexane and EtOAc.

Laboratory analysis of trial T6

Organic impurities were removed from the obtained reacting acid solution by filtering. Then, the formed crystals were filtered and washed with ethanol (1 x 100 mL) to obtain colourless crystals (17.1 g, fraction 1). The filtrate was transferred partly into a 1000 mL round flask for removing water *in vacuo*. Besides, crystallization was observed in another portion of the filtrate that had not been transferred into the round flask. The water removal process in the 1000 mL round flask was halted to promote crystallization. As anticipated, about 15 min after removing the solution from the rotary evaporator, crystallization occurred within the round flask. The formed crystals were filtered and washed with ethanol (3 x 50 mL) to yield colourless crystals

(97.5 g, fraction 2). The filtrate was transferred into a 500 mL round flask to remove the water *in vacuo* altogether. The obtained solid was washed with ethanol (3 x 50 mL), then with ethyl acetate (1 x 80 mL) to yield a white solid (60.8 g, fraction 3).

Trial 7 (Recrystallization)

The obtained product of T4 (100 g) was dissolved in deionised water (300 mL) at 30 °C. The emerged foam was removed. The water was then removed *in vacuo* (p = 380 mbar, T = 95 °C). Subsequently, the supersaturation grad was determined by measuring the condensed liquid in the collecting flask. After 1.5 h, 90 mL of condensed water was obtained in the collecting flask. With the supersaturation of 1.3, the MAP nucleation was carried out. The hot solution was transferred to a metal tablet (30 cm x 20 cm), and analytical MAP (0.5 g) was evenly implied over the tablet. After 10 min, definitive crystal growth was observed that was allowed to crystallise overnight. The obtained crystals were filtered and washed with ethanol (30 mL) to yield colourless crystals (87.3 g).

Laboratory analysis of trial T8

Firstly, the fillers were filtered with impurities. In order to achieve a certain level of supersaturation and estimate the potential amount of MAP that could be obtained, the water was evaporated at p = 300 mbar and a temperature (T = 95 °C) for 1 hour. Afterwards, 320 mL of condensed water was measured in the collecting flask. The crystal growth was conducted overnight (see T7). The obtained crystals were filtered and washed with ethanol (2 x 50 mL). The filtrate was filtered again to obtain the precipitated solid, yielding pink crystals and a white solid (144.1 g).

Trial T9 - Ammonia recovery from TCR® water

T9.1. Using phosphoric acid 85%

The experimental setup is shown in Figure 13.

The TCR® water (400 mL) was filled in a 1000 mL four-neck round flask. The dropping funnel was filled with concentrated sodium hydroxide solution in excess (50 mL, 10 M). The washing bottles (6) and (8) were filled with concentrated phosphoric acid 85% (17.3 M, 105 mL) and 4.0 M (80 mL), respectively. The washing bottle (9) was filled with phenolphthalein (0.1 wt-% in ethanol). To start the experiment, the heating temperature was set at 150 °C. NaOH solution (50 mL, 10 M) was added dropwise under stirring into the TCR® water in 1 h.

T9.1. Using phosphoric acid 4.0 M

The experimental setup is shown in Figure 15. All the solutions were prepared as same as T9.1 except that the washing bottles (6) were filled with dilute phosphoric acid (4.0 M, 120 mL).

The washing bottles (6) of both attempts were combined and the water was removed partly *in vacuo* for 1 h. The crystal growth was conducted overnight (see T7). The obtained crystals were filtered and washed with ethanol (2 x 50 mL) to yield pink crystals and a white solid (98.4 g).

List of Tables

Table 1: Operate conditions of different thermal conversion processes and the typical product weight yields with dry wood as feedstock.[9, 12-13] 8
Table 2: Overview of all ammonia recovery units used in this work, which were carried out with different feedstocks at different post-reforming temperatures..... 16
Table 3: Calculation of overall yields and conversion rates (CR: conversion rate). The same colour of the trials indicates the same/similar feedstocks. 17
Table 4: Percent compositions of nitrogen, hydrogen, carbon, and sulfur in pure MAP compared with the obtained products of T1 – T9..... 18
Table 5: TCR® gas composition at 700 °C reforming temperature in T1. 20
Table 6: Results of the elementary analysis of three fraction in T6. 27
Table 7: The obtained MAP before (left) and after (right) the recrystallization. 29
Table 8: Analytical results of obtained product in T9 34

List of Figures

Figure 1: Schematic of the TCR® reactor. (©Fraunhofer UMSICHT) 10
Figure 2: The natural nitrogen cycle. [26-27] 11
Figure 3: TCR®-2 plant at the ©Fraunhofer Institute UMSICHT, Sulzbach-Rosenberg with the components: (1) metal bunker, (2) vision panel, (3)(10) screw reactors, (4) auger reactor for pyrolysis, (5) post-reformer, (6) condenser, (7) electrostatic cyclone precipitator (ECP), (8) collecting glass bottles for condensate, (9) wash bottle, (11) char collecting tank, (12) bypasses. 13
Figure 4: The precipitation experiment of the sample from bypass 1 with acetone in a ratio of (left to right) 1:25, 1:30, 1:35, 1:40, 1:45, 1:50, 1:55, 1:60, and 1:70. 19
Figure 5: Formed colourless precipitation..... 19
Figure 6: chemical structures of a) pyrrole. b) porphin, the parent porphyrin 21
Figure 7: Brown lumps formed during water evaporation. 22
Figure 8: a) hop spent grain pellets, b) Foam formation in the bypasses during trial T3. 23
Figure 9: a) Organic impurity was dissolved in EtOAc (left) and n-hexane (right), b) liquid-liquid-extraction of the obtained product (right) in water with different solvents, from left: THF, n-hexane, EtOAc..... 26
Figure 10: Formed crystals in trial 6. 27
Figure 11: The obtained MAP in three fractions: fraction 1 (left), fraction 2 (middle), and fraction 3 (right). 27
Figure 12: Crystal growth observation: a) at the beginning, b) after 10 min, c) after 30 min, d) overnight. 28
Figure 13: Experimental setup (T9.1) for ammonia recovery from TCR® water: (1) four-neck round flask, (2) dropping funnel, (3) thermometer, (4) heating mantel, (5) plastic tubes, (6) washing bottle filled with phosphoric acid 60% and plastic fillers, (7) ice bath, (8) washing bottle filled with phosphoric acid 35% and plastic fillers, (9) washing bottle filled with phenolphthalein 1 wt-% in ethanol..... 31
Figure 14: The colour change of the acid solution during the ammonia absorption every 2 minutes (left to right) 32
Figure 15: Experimental setup (T9.2) for ammonia recovery from TCR® water: (1) four-neck round flask, (2) dropping funnel, (3) thermometer, (4) heating mantel, (5) plastic tubes, (6) washing bottle filled with phosphoric acid 35% and plastic fillers, (7) ice bath, (8) washing bottle filled with phenolphthalein 1 wt-% in ethanol. 33

References

[1] L. Bird, D. Lew, M. Milligan, E. M. Carlini, A. Estanqueiro, D. Flynn, E. Gomez-Lazaro, H. Holttinen, N. Menemenlis, A. Orths, *Renew. Sust. Energ. Rev.* **2016**, *65*, 577-586.

[2] R. Bekker, N. M. Prinsloo, *Ind. Eng. Chem. Res.* **2009**, *48*, 10156-10162.

[3] J. Neumann, J. Meyer, M. Ouadi, A. Apfelbacher, S. Binder, A. Hornung, *Waste Manage.* **2016**, *47*, 141-148.

[4] H. Jørgensen, J. B. Kristensen, C. Felby, *Biofuel Bioprod Biorefin* **2007**, *1*, 119-134.

[5] Y. Lin, S. Tanaka, *Appl. Microbiol. Biotechnol.* **2006**, *69*, 627-642.

[6] A. Molino, F. Nanna, Y. Ding, B. Bikson, G. Braccio, *Fuel* **2013**, *103*, 1003-1009.

[7] T. Bridgwater, *J. Sci. Food Agric.* **2006**, *86*, 1755-1768.

[8] T. BRIDGWATER, K. Maniatis, *Molecular to global photosynthesis*, World Scientific, **2004**, 521-611.

[9] A. Hornung, *Transformation of biomass: theory to practice*, John Wiley & Sons, **2014**.

[10] H. Goyal, D. Seal, R. Saxena, *Renew. Sust. Energ. Rev.* **2008**, *12*, 504-517.

[11] S. Czernik, A. Bridgwater, *Energy Fuels* **2004**, *18*, 590-598.

[12] A. V. Bridgwater, *Biomass Bioenergy* **2012**, *38*, 68-94.

[13] N. Schmitt, A. Apfelbacher, N. Jäger, R. Daschner, F. Stenzel, A. Hornung, *Biofuel Bioprod. Biorefin.* **2019**, *13*, 822-837.

[14] M. Kratzeisen, N. Starcevic, M. Martinov, C. Maurer, J. Müller, *Fuel* **2010**, *89*, 2544-2548.

[15] D. Meier, *Wirtschaftliche Realisierung der Flashpyrolyse von Altholz mit anschließender energetischer Verwertung in einem BHKW*, can be found under https://policycommons.net/artifacts/2652338/wirtschaftliche-realisierung-der-flashpyrolyse-von-altholz-mit-anschliessender-energetischer-verwertung-in-einem-bhkw/3675211/, **2007**.

[16] Z. Luo, S. Wang, Y. Liao, J. Zhou, Y. Gu, K. Cen, *Biomass Bioenergy* **2004**, *26*, 455-462.

[17] Q. Zhang, J. Chang, T. Wang, Y. Xu, *Energy Convers. Manag.* **2007**, *48*, 87-92.

[18] S. Binder, M. Jakuttis, A. Apfelbacher, A. Hornung, Google Patents, **2018**.

[19] A. Hornung, A. Apfelbacher, S. Sagi, **2011**.

[20] A. Hornung, *Biomass Combustion Science, Technology and Engineering: 8. Intermediate Pyrolysis of Biomass*, Elsevier Inc. Chapters, **2013**.

[21] A. S. Mahmood, J. G. Brammer, A. Hornung, A. Steele, S. Poulston, *J. Anal. Appl. Pyrolysis* **2013**, *103*, 328-342.

[22] A. Hornung, A. Apfelbacher, J. Neumann, N. Jäger, N. Schmitt, R. Daschner, EUBCE, **2016**.

[23] E. Ahmad, N. Jäger, A. Apfelbacher, R. Daschner, A. Hornung, K. Pant, *Fuel Process. Technol.* **2018**, *171*, 277-286.

[24] J. Neumann, S. Binder, A. Apfelbacher, J. R. Gasson, P. R. García, A. Hornung, *J. Anal. Appl. Pyrolysis* **2015**, *113*, 137-142.

[25] J. Karl, *Dezentrale Energiesysteme 3. A. Neue Technologien im liberalisierten Energiemarkt*, Oldenbourg Wissenschaftsverlag, **2012**.

[26] H. Lehn, H. Flaig, H. Mohr, *GAIA-Ecological Perspectives for Science and Society* **1995**, *4*, 13-25.

[27] H. Mohr, P. Schopfer, H. Mohr, P. Schopfer, *Plant Physiol.* **1992**, 155-194.

[28] G. Sekhon, *J. Contam. Hydrol.* **1995**, *20*, 167-184.

[29] B. Singh, G. Sekhon, *Agric. Environ.* **1979**, *4*, 207-225.

[30] R. Conti, N. Jäger, J. Neumann, A. Apfelbacher, R. Daschner, A. Hornung, *Energ. Technol.* **2017**, *5*, 104-110.

[31] IEA, *Ammonia Technology Roadmap*, can be found under https://www.iea.org/reports/ammonia-technology-roadmap, **2021**

[32] M. J. Matzen, M. H. Alhajji, Y. Demirel, *J. Adv. Chem. Eng.* **2015**, 5:3.

[33] S. Ghavam, M. Vahdati, I. G. Wilson, P. Styring, *Front. Energy Res.* **2021**, *9*, 580808.

[34] F. Haber, *Nobel Lecture* **1920**, *2*.

[35] J. W. Erisman, M. A. Sutton, J. Galloway, Z. Klimont, W. Winiwarter, *Nat. Geosci.* **2008**, *1*, 636-639.

[36] D. Dong, O. K. Choi, K. Lee, Y. Hong, J. W. Lee, *J. Mater. Cycles Waste Manag.* **2018**, *20*, 578-584.

[37] International Plant Nutrition Institute (IPNI), *Nutrient Source Specifics (No.9), Monoammonium Phosphate (MAP),* can be found under http://www.ipni.net/publication/nss.nsf/0/2F200FA9C8C946F0852579AF00762904/$FILE/NSS-09%20Monoammonium%20Phosphate.pdf, **2019**

[38] D. Xu, X. Xiong, L. Yang, Z. Zhang, X. Wang, *J. Chem. Eng. Data* **2016**, *61*, 78-82.

[39] M. Gargouri, V. Chtara, P. Sharrock, A. Nzihou, H. Feki, *Int. J. Mater. Eng.* **2012**, *2*, 32-37.

[40] L. Luskar, J. Polanšek, A. Hladnik, B. Čeh, *Appl. Sci.* **2022**, *12*, 4190.

[41] B. Eghball, J. F. Power, J. E. Gilley, J. W. Doran, Wiley Online Library, **1997**.

[42] E. Halbig, Master thesis, Nuremberg Institute of Technology Georg Simon Ohm **2022**.

[43] A. de Klerk, *Catalysis* **2011**, *23*, 1-49.

[44] G. Egloff, *J. Ind. Eng. Chem.* **1936**, *28*, 1461-1467.

[45] P. Rothemund, *J. Am. Chem. Soc.* **1935**, *57*, 2010-2011.

[46] H. A. Raza, Master thesis, Otto von Guericke University Magdeburg **2021**.

[47] R. Schlögl, *Angew. Chem.* **2003**, *115*, 2050-2055.

[48] J. Nessler, *Chem. Centr.* **1856**, *27 (neue Folge 1, Band I)*, 529.

[49] F. J. Krug, J. Růžička, E. Hansen, *Analyst* **1979**, *104*, 47-54.

[50] ChemicalBook, *Ammonium dihydrogen phosphate*, can be found under https://www.chemicalbook.com/ChemicalProductProperty_EN_CB6131092.htm

[51] Bundesinstitut für Risikobewertung, *Polyzyklische aromatische Kohlenwasserstoffe (PAK) in Spielzeug*, can be found under https://www.bfr.bund.de/cm/343/polyzyklische_aromatische_kohlenwasserstoffe_pak_in_spielzeug.pdf, **2009**.

[52] S. Kuppusamy, P. Thavamani, K. Venkateswarlu, Y. B. Lee, R. Naidu, M. Megharaj, *Chemosphere* **2017**, *168*, 944-968.

[53] X.-Y. Lu, T. Zhang, H. H.-P. Fang, *Appl. Microbiol. Biotechnol.* **2011**, *89*, 1357-1371.

[54] J.-C. Charpentier, *Adv. Chem. Eng., Vol. 11*, Elsevier, **1981**, 1-133.

[55] N. Doki, N. Kubota, M. Yokota, S. Kimura, S. Sasaki, *J. Chem. Eng. Japan* **2002**, *35*, 1099-1104.

[56] H. Oosterhof, G. Witkamp, G. Van Rosmalen, *Fluid Ph. Equilibria.* **1999**, *155*, 219-227.

[57] D. Xu, D. Xue, H. Ratajczak, *J. Mol. Struct.* **2005**, *740*, 37-45.

[58] S. Urréjola, A. Sánchez, M. n. F. Hervello, *J. Chem. Eng. Data* **2011**, *56*, 2687-2691.

[59] H. Oosterhof, G. J. Witkamp, G. M. van Rosmalen, *AIChE J.* **2001**, *47*, 602-608.